scientific reports

Check for updates

OPEN

First dercetid fish from the Upper Cretaceous of Antarctica

Valéria Gallo[1]✉, Francisco J. de Figueiredo[1], Arthur Souza Brum[1]✉, Marina Bento Soares[3], Juliana Manso Sayão[2,3], André Eduardo Piacentini Pinheiro[4], Rodrigo Giesta Figueiredo[5], Ricardo Tadeu Lopes[6], Olga Maria Oliveira de Araújo[6] & Alexander W. A. Kellner[3]

Aulopiformes, a clade including lizardfishes and allies, comprise a long-standing marine lineage from the Early Cretaceous to the Recent. We describe *Antarctichthys longipectoralis* gen. et sp. nov. from the late Campanian marine strata of Antarctica (Snow Hill Island Formation). This species, represented by a single specimen, was recovered during the expedition of PALEOANTAR in Santa Marta Cove (James Ross Island) and it is the most complete vertebrate found in this locality, with a three-dimensional preservation. It was microCT-scanned, providing exclusive details on the anatomy of Aulopiformes unknown for the early history of the clade, i.e., an unexpected otophysic connection in the neurocranium. It has been classified within Dercetidae due to the presence of a longirostrine head, an elongated body, and very reduced neural spines (their unequivocal synapomorphy). It is distinguished from all known dercetids by its elongated pectoral fin and the absence of teeth. Phylogenetic analysis placed it as sister-genus to the late-diverging clade *Rhynchodercetis* plus *Hastichthys*. The earliest occurrence of Dercetidae is recorded in the lower Cenomanian, from Komen, Jebel Tselfat and Ein-Yabrud. The pivotal record of this new dercetid fish in Antarctica marks the southernmost occurrence of the group, previously known from the Pelotas Basin, Southern Brazil.

Fossil aulopiforms have been discovered in many sedimentary deposits across almost all continents—North and South America, Europe, Asia and Africa[1]—, but they are rare in Antarctica[2]. The living taxa are morphologically and ecologically diverse, ranging from benthic to pelagic forms, and inhabiting environments from coastal regions to deep oceanic abysses (>3,000 m deep). Like other late-diverging teleosts, their intra- and interrelationships are far from a consensus. Aulopiformes encompass 5 suborders, 24 families, 78 genera (e.g.,[3–7]) and ~330 species.

The fossil family Dercetidae includes marine, long-snouted teleosts with elongated, shallow body, bearing one or more rows of tripartite scutes along the flanks and one or two pairs of prominent transverse processes on each abdominal vertebral centrum. It is commonly found in Tethyan deposits of Europe, Asia, and Africa, ranging from the Late Cretaceous (Cenomanian) to the Paleocene (Danian[8]). The taxonomic status of certain genera and species within Dercetidae remains problematic. However, several taxa are regarded as valid according to studies by Silva & Gallo[1], Taverne & Goolaerts[9], Alvarado-Ortega & Díaz-Cruz[10], Chida et al.[8], and a comprehensive list is provided by Alvarado-Ortega & Díaz-Cruz[10].

Fossil fish from James Ross Island (JRI; Antarctica) have been known since the early twentieth century[11] and includes holocephalians, selachians, and bony fishes[2,11–22]. Among the bony fishes, most records comprise by isolated and fragmentary material. Aulopiformes specimens from JRI are restricted to the late Campanian–Maastrichtian sequences, with known occurrences including Sphenocephalidae, *Apateodus* and *Enchodus*[2,15,23].

Here, we describe the first three-dimensional dercetid fish, from the Snow Hill Island Formation, late Campanian marine strata of Antarctica.

Systematic Paleontology

Teleostei Müller, 1845

Neoteleostei Nelson, 1969

Aulopiformes Rosen, 1973

Enchodontoidei sensu Silva and Gallo, 2011

[1]Departamento de Zoologia, Universidade do Estado do Rio de Janeiro (UERJ), Rio de Janeiro, RJ, Brazil. [2]Programa de Pós-Graduação em Zoologia, Museu Nacional-Universidade Federal do Rio de Janeiro (MN-UFRJ), Rio de Janeiro, RJ, Brazil. [3]Laboratório de Paleobiologia e Paleogeografia Antártica, Departamento de Geologia e Paleontologia, MN-UFRJ, Rio de Janeiro, RJ, Brazil. [4]Faculdade de Formação de Professores, UERJ, Campus São Gonçalo, São Gonçalo, RJ, Brazil. [5]Departamento de Biologia, Universidade Federal do Espírito Santo, Alegre, ES, Brazil. [6]Laboratório de Instrumentação Nuclear, Programa de Engenharia Nuclear, UFRJ, Rio de Janeiro, RJ, Brazil. ✉email: gallo@uerj.br; arthur7sbc@gmail.com

Dercetidae Woodward, 1901

Antarctichthys gen. nov.

Derivatio nominis. From the Greek word αντι, *anti-* meaning in opposite of, αρκτός, *arktos- meaning* north and *Ιχθύς*, *ichthus-* meaning fish.

Type and only known species. *Antarctichthys longipectoralis* sp. nov.

Diagnosis. A small-sized dercetid fish diagnosed by a unique combination of characters, some of them being autapomorphies (*): snout longer than the lower jaw; absence of teeth (*); most of dermal bones of skull roof and opercular series smooth; parietal ornamented with straight and parallel striae (*); lateroparietal skull roof; small autosphenotic with a reduced spine-like process and a shallow dilatator fossa; elongated pterotic extending beyond the level of the occiput region; foramina for the hyomandibular trunk and orbital artery closely associated; jugular vein canal present; very elongated parasphenoid with a broad and low ascending process; stout basipterygoid process (*); otic bulla absent; presence of otophysic connection through exoccipital foramen (*); exoccipitals delimiting a large campaniform foramen magnum, ventrally separated by the basioccipital; foramen for the glossopharyngeal nerve located near the contact zone between exoccipital and prootic (*); basioccipital with a long notochordal canal extending forward (*); *Cyranichthy*s-like opercle; narrow and boomerang-shaped preopercle; scapular foramen placed in the junction of scapula and cleithrum; very elongated and stout pectoral fin-rays (*); spoon-shaped vertebral centra with very large notochordal foramen; neural arches large and deep as the centra; first and second centra with a unique well-developed wing-like transverse process; third to the last preserved centra with enlarged and sharp anterior transverse process and atrophied posterior transverse process; scutes absent.

Antarctichthys longipectoralis sp. nov.

(Fig. 1)

LSID. zoobank.org:pub:6239D9F9-BDDE-4D80-922D-C1D078AD165C.

Derivatio nominis. From the Latin words '*longus*' (meaning long) and '*pectoralis*' (meaning pectoral), an allusion to the larger size of the pectoral fin compared to other known species.

Holotype. MN 7838-V.

Stratigraphic range. The specimen MN 7838-V was recovered during the PALEOANTAR expedition at Santa Marta Cove, James Ross Island, during the austral summer of 2018/2019, as part of the 37th Antarctic Operation (OPERANTAR XXXVII). The fossil was found in a heavily eroded area, embedded within a small fossiliferous deposit of fine-grained sand located at coordinates 63°54′13.9"S; 57°55′04.7"W. It represents the upper Campanian deposits[24] of the Snow Hill Island Formation, near the Shark Stream and across from the San José Glacier.

Palaeoenvironment. Shoreface-offshore marine.

Diagnosis. As for the genus.

Description

The holotype is a single and incomplete specimen, preserved with most of the body twisted and embedded within the calcareous matrix (Fig. 1). The vertebral column is mostly articulated but some elements are detached and individualized. As typical of dercetid fishes, the body is very long and slender, and the head produces a prominent snout. The caudal fin and most of the rostrum are not preserved so that the standard length is unknown. Based on the conservative morphology of better-known dercetids and the preserved skull and articulated vertebrae, *Antarctichthys* is likely the smallest dercetid taxon. The braincase is well ossified, with few cartilaginous interspaces in its walls indicating an adult fish; the same for number of fin-rays articles. Pelvic, dorsal, and anal fins were not preserved, but there are very elongate pectoral fin-rays, which are larger than that of *Dercetis*, and seems to be positioned high on the flanks. The body lacks scales, and scutes are not observed.

The skull roof is partially preserved in dorsal view, with roofing bones that are thin and laminate. These bones are smooth except for the extrascapular bone, which is ornamented. Although the snout is incomplete, with only the mesethmoid and a portion of the frontals remaining in a joined set, it seems to be very long and pointed, a common feature among dercetids. The length from the vomer to the pterotic spine spans approximately 8–9 vertebrae. The orbit diameter is about one-eighth of the vomer-parietal length. Some chondral bones from the otic and occipital regions are slightly disarticulated and displaced, likely due to fossil diagenesis (Fig. 1f).

A displaced, elongate, thin bony sheet is interpreted as the supraethmoid. Its length is approximately three times that of the centra. The anterior end is enlarged and truncated, with digitate lateroventral process to receive the palatine and few anteriorly laterodorsal process to meet the upper jaw. Its dorsal surface has a convex profile and ventrally it shows a deep internal cavity extending forward, which may have been filled with cartilage in life. The posterior end of the bone is acute to fit the frontals, and this joint point is placed very far from the anterior border of the orbit. Below the cartilage block, a thin ypsiloid bone is interpreted as the hypoethmoid. The olfactory organ was likely well developed due to the large space between the lateral ethmoid and the supraethmoid-frontal joint.

The lateral ethmoid is a well-ossified, triangular bone in lateral view, sutured to the ventral surface of the frontal. It forms the anterior limit of the orbit and most of its dorsal border. Ventrally, this bone appears to contact the parasphenoid.

The nasal is small and slender, positioned laterally to the frontal, with the supraorbital sensory canal running along its midline in a straight and fine tubular relief.

The frontal is the largest bone in the skull roof, very elongate and narrow above the orbit and anterior to it. Posterior to the orbit, the frontal has a convex profile and become expanded laterally. Both frontals are joined to each other by a straight suture and are almost complete, except for their anteriormost ends at the level of mesethmoid in which they are broken. Posteriorly, the frontals contact the parietals through a gently curved

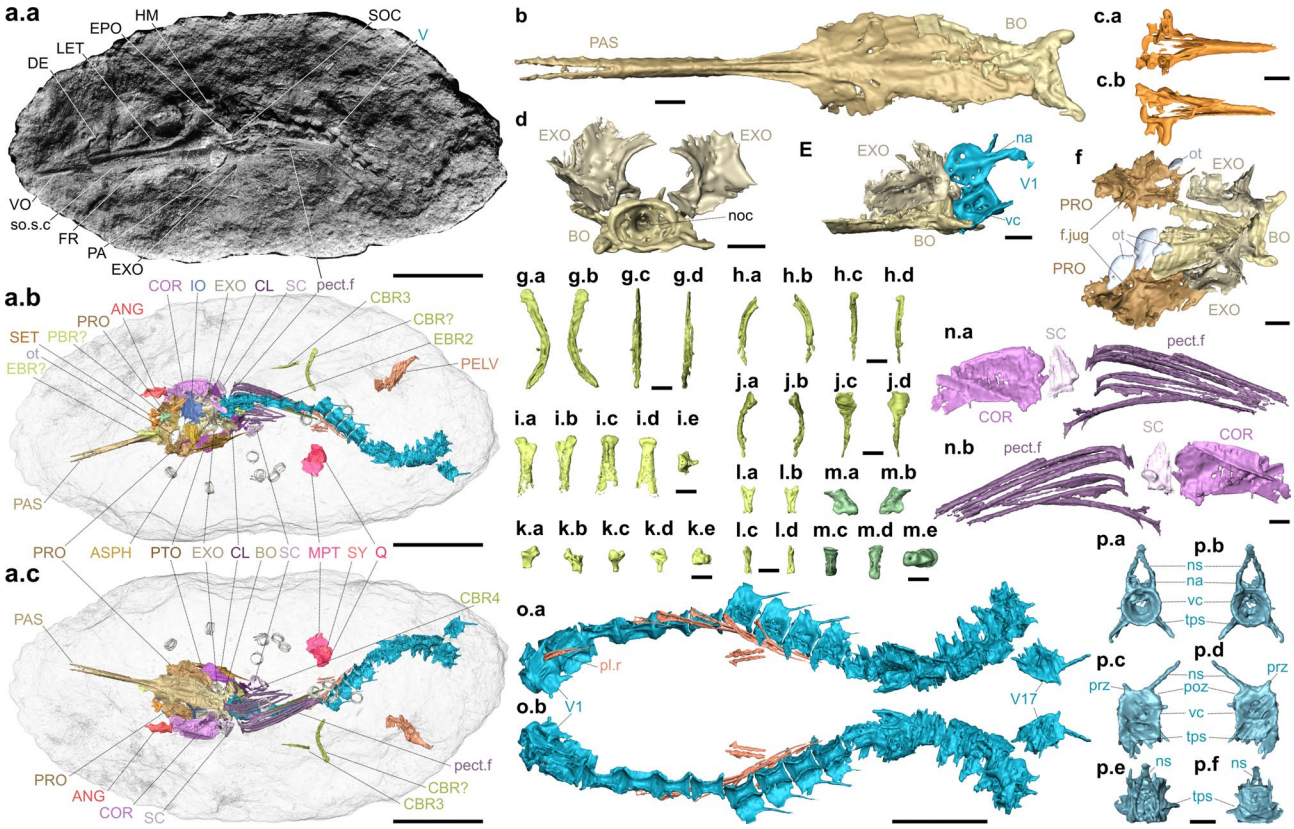

Fig. 1. Holotype of *Antarctichthys longipectoralis* from the Snow Hill Island Formation, Upper Cretaceous of Antarctica. Photograph of the external surface of the specimen (**A.a**) and rendering of the bones inside the bone matrix in dorsal (**A.b**) and ventral views (**A.c**). The articulated parasphenoid and basioccipital in ventral view (**B**). The supraethmoid in dorsal (**C.a**) and ventral views (**C.b**). The articulation between the exoccipitals and basioccipital in posterior view (**D**). The articulation between the exoccipital, basioccipital and the first vertebra in left lateral view (**E**). The articulation between the prootics, exoccipitals and basioccipital in dorsal view (**F**). Right ceratobranchial in anterior (**G.a**), posterior (**G.b**), medial (**G.c**), and lateral (**G.d**). Right third ceratobranchial in anterior (**H.a**), posterior (**H.b**), medial (**H.c**), and lateral (**H.d**). Right indeterminate epibranchial in anterior (**I.a**), posterior (**I.b**), medial (**I.c**), lateral (**I.d**), and articular (**I.e**). Right fourth ceratobranchial in anterior (**J.a**), posterior (**J.b**), medial (**J.c**), and lateral (**J.d**). Right second epibranchial in (**K.a**), posterior (**K.b**), medial (**K.c**), lateral (**K.d**), and articular (**K.e**). Right indeterminate epibranchial in anterior (**L.a**), posterior (**L.b**), medial (**L.c**), and lateral (**L.d**). Left indeterminate pharingobranchial in anterior (**M.a**), posterior (**M.b**), medial (**M.c**), and lateral (**M.d**). The right pectoral girdle and fins, with the semi-articulation between coracoid, scapula and pectoral fins in medial (**N.a**) and lateral views (**N.b**). Vertebral series in articulation from first to 17th vertebra in ventral (**O.a**) and dorsal views (**O.b**). The 17th vertebra in anterior (**P.a**), posterior (**P.b**), left lateral (**P.c**), right lateral (**P.d**), dorsal (**P.e**), and ventral (**P.f**). Abbreviations: ANG, anguloarticular; ASPH, autosphenotic; CBR, ceratobranchial; CL, cleithrum; COR, coracoid; EBR, epibranchial; EPO, epioccipital; EXO, exoccipital; f.jug, jugular foramen; FR, frontal; HM, hyomandibula; IO, infraorbital; LET, lateral ethmoid; MPT, metapterygoid; na, neural arch; noc, notochordal canal; ns, neural spine; ot, otolith; PA, parietal; PAS, parasphenoid; PBR, pharingobranchial; pect.f, pectoral fins; PELV, pelvic bones; pl.r, pleural rib; poz, postzygapophysis; PRO, prootic; prz, prezygapophysis; PTO, pterotic; Q, quadrate; SC, scapula; SET, supraethmoid; SOC, supraoccipital; so.s.c, supraorbital sensory canal; SY, symplectic; tps, transverse process; V, vertebra; vc, vertebral centrum; VO, vomer. Scale bars equal to 10 mm in A, 1 mm in B-N and P, and 5 mm in O.

suture. The trajectory of the supraorbital sensory canal is straight along most of the bone, except in the postorbital region at the level of the autosphenotic, in which the canal curves laterally toward the pterotic.

The small falcate parietal is finely ornamented with straight and parallel striae. The bones are separated by the supraoccipital, generating a lateroparietal condition of the skull roof. Each parietal contacts the pterotic laterally and the epioccipital posteriorly.

The autosphenotic is a small triangular bone in lateral view, bearing a small spine-like process. It is overlapped by the frontal and meets the pterosphenoid anteriorly, the pterotic posteriorly, and the prootic ventrally. The autosphenotic, along with the frontal, forms the posterodorsal corner of the orbit and contributes with a reduced portion for a shallow dilatator fossa. Dorsally, there is a minute foramen for the otic branch of the facial nerve. Its inner fine perichondral wall lodges the anterodorsal loop of the anterior semicircular duct.

The pterotic is an elongated and relatively narrow bone, with a subrectangular shape dorsally and an anterodorsal arm contacting the autosphenotic. The bone projects backward in an acute spine that extends beyond the level of the occiput region. The trajectory of the otic sensory canal is marked by a groove on the anterodorsal arm of the pterotic and a tubular relief on the main body of the bone. It has a long and shallow articular facet for the hyomandibula, which seems continuous with the autosphenotic. The pterotic contacts the exoccipital through a long rectilinear suture. The post-temporal fossa is shallow and appears to be unroofed. The internal face of the pterotic has a lateral arch for the passage of the horizontal semicircular canal.

The prootic is the most complex bone of the braincase, appearing subrectangular in lateral view. Each one is displaced from their anatomical position, so it is preserved slightly inclined. Thus, the short and slender prootic bridge is descontinuous. The cavity floor of the otic skull is anteriorly bordered by the prootic bridge and posteriorly by the basioccipital. The lateral face of the prootic is pierced by three foramina. Dorsally, there is a moderate foramen for the exit of the hyomandibular trunk of the facial nerve; ventrally, a foramen for the entrance of the orbital and orbitonasal arteries; posteriorly, there is a posterior opening of jugular canal. The foramina for the hyomandibular trunk and orbital artery are closely associated as in the living *Synodus* (pers. obs.). Furthermore, there is an anterodorsal minute foramen for the exit of the ascending branch of the hyomandibular trunk toward the orbital region. The lateral face of the prootic bears an arched ridge beneath the subtemporal fossa.

On the anterior face, the prootic lodges the *trigeminofacialis* chamber. There is a large foramen including trigeminal and anterior opening of jugular canal. This foramen is ventrally open, probably bordered by cartilage medially and associated with an anterior finger-like outgrowth of the prootic. The *pars jugularis* is elongate and the *pars ganglionaris* corresponds to a shallow recess on the medial face of the prootic. The jugular vein runs through a long canal along the lateral border of the prootic, originating at the middle portion of the bone.

Dorsomedially, near the contact with the autosphenotic, there is a tiny foramen for the otic branch of facial nerve. Dorsally, the anterodorsal portion of the prootic has a large platform, probably overlain by the lateral expansion of the frontal. Posterior to the *trigeminofacialis* chamber, at the junction with the autosphenotic, the prootic produces a low *recessus utriculi*. Laterally, prootics and pterotics contact to form the wall of the otic cavity. The prootic-intercalar bridge is absent. The trigeminal foramen is large and exposed both dorsally and ventrally to the chamber. It is separated from the large facial foramen by a spicular bony commissure. Posterior to the trigeminal foramen, there is an elongate strut splitting superior and inferior portions of inner ear.

A trapezoidal pterosphenoid is preserved medial to the autosphenotic and ventral to the prootic. Dorsally, it has a platform to receive the ventral portion of the frontal; anteriorly, it forms the posterior wall of the orbital fenestra. Medially, near the dorsolateral border of the cranial cavity, the foramen for the trochlear nerve is situated, with upper and lower grooves and foramina for the recurrent branch of the facial nerve and the middle cerebral vein nearby. Ventrally, a notch accommodates the basisphenoid (not preserved). A large shield-like plate in the inner orbital region is interpreted as the orbitosphenoid.

The vomer is short, fusiform, and toothless. It contacts the parasphenoid anterior to the orbit, about four times the orbit diameter. Mediodorsally, the vomer extends a keel to the mesethmoid.

The parasphenoid is very elongated—eight times the vertebral centrum length. It tapers forward below the orbit, bifurcating at the anterior end to receive the vomer medially. At the level of the posterior border of the orbit, the parasphenoid projects a broad and low ascending process that meets the prootic through a nearly straight suture. At the hind edge of the orbit, it bears lateroventrally a stout basipterygoid process. In ventral view, the large foramen for the internal carotid artery lies medial to this process. Dorsally, a slender bony bridge anterior to this foramen splits the efferent pseudobranchial and ophthalmic magna arteries. The efferent pseudobranchial artery runs forwards in a deep and straight excavation on the ascending process.

Posterior to the prootic bridge, there is a long median shelf on upper surface of parasphenoid forming the floor of the posterior myodome and, dividing each side, there is a deep and elongate groove towards the basioccipital. The parasphenoid is posteriorly flat and bifurcates to contact the basioccipital, which apparently opens to the myodome posteriorly, rather than forming an otic bulla.

The exoccipital forms most of the posterior braincase in lateral view. Apparently, it meets its antimere above the large campaniform foramen magnum through a thickened buttress (the arched superior vertical lamina sensu Kesteven, 1928), that forms its lateral border. Seemingly, the exocciptals are surmounted by the supraoccipital. Ventrally, the exoccipitals meet the basioccipital, which interrupts the contact between these paired bones with each other. Internally, the exoccipitals form the postotic wall. Posteromedially, in its occipital segment, the exoccipital produces a horizontal lamina to meet the basioccipital and in front of this there is a large vertical window corresponding to the opening of the chamber to the posterior ampulla of the inner ear. Together with the lateral lamina of the basioccipital, the ventral margin of the posterior portion of the exoccipital forms the posterior wall of the otolith chamber. The exoccipitals contribute a little with small occipital condyles flanking the foramen magnum and lying above the basioccipital condyle.

The anterodorsal region of the exoccipital, along with the adjacent concavity of the prootic, forms a shallow depression—the subtemporal fossa—, likely associated with the extension of the *adductor hyomandibulae* muscle. On the outer surface of exoccipital, a curved laminar outgrowth serves as the attachment for the intercalar bone (not preserved).

The foramen for the glossopharyngeal nerve is located near the exoccipital-prootic contact. Internally, the foramen is associated to an opening into a strut forming the lateral border of the otic portion of the otolith chamber.

The large foramen for the vagus nerve opens ventrolaterally and upward into a groove at the exoccipital that housed the supratemporal branch of this nerve. A nearby auditory fenestra, likely covered by a connective membrane in life, is located mid-ventrally on the exoccipital. Both openings are separated by a vagus-auditory

laminar outgrowth. The auditory fenestra is associated to the saccule to receive the cranial diverticulum from the swim bladder.

The posterior region of the exoccipital bears two foramina for occipital nerves closely associated to the superior vertical lamina of the bone.

The basioccipital forms the posterior portion of the floor of the cranial cavity. Its dorsal border forms the floor of the foramen magnum. Laterally, the bone bears prominent accessory process on each side, probably for Baudelot's ligament. Anteromedially, the bone slopes downwards producing a deep excavation, which might lodged the *sinus impar perilymphaticus*. Along with the exoccipital, the basioccipital forms a reduced lagenar chamber for asteriscus otolith (not preserved). In front of it, this bone forms the walls of the posterior parts of the saccular and utricular chambers. A low median platform arising from the ventral surface of the bone divides the paired otolith chambers and its medioventral cavity corresponds to the posterior limit of the myodome. Anteriorly, there is a large space that communicates with the otolith chambers and the myodome. Ventrally this bone projects two parallel crests, delimiting an aortic groove. The bone ends in a basioccipital facet of occipital condyle, and near it and below the first vertebral centrum is noted a pair of small chevron-like bony pieces that seems to support the dorsal aorta. A long notochordal canal extends forwards, gradually tapering until reaches the myodome chamber through a reduced pit.

The left epioccipital is preserved but displaced from its anatomical position. It is a squarish and deeply excavated bone, with a reduced surface for the dorsal arm of the post-temporal bone. The right epioccipital is seen externally but its poor preservation hampers an adequate description.

The large triangular supraoccipital has a low median crest. It splits medially the parietals, producing the so-called lateroparietal condition of the skull roof. It is bordered by the epioccipitals.

Only the right extrascapular is preserved as a subrectangular and elongate bone. It bears a straight supratemporal commissural sensory canal crossing the bone length.

The otoliths include a pair of *sagitta* and a pair of *lapillus*. The *sagitta* is oblong in shape and moderate in size with smooth borders. It has reduced notches for *excisura ostii*, fading dorsal and ventral cristae, and short *ostium* and *cauda* in the *sulcus acusticus*. The *rostrum* is prominent, whereas the *antirostrum* is absent. The *lapillus* is rounded and much smaller, fitting, at least, three times in the *sagitta* length. The anterior extremity is continuous without *excisura*. Both anterior and posterior extremities have a globose shape. Seemingly, dorsal and ventral borders are smooth. It bears a reduced *gibbus maculae*.

From the circumorbital series, apparently only the antorbital and the fifth infraorbital are preserved. The large posterior infraorbitals, judging by the space between the orbit and preopercle, likely expanded to cover the hyomandibula. A small kidney-shaped impression anterior to the lateral ethmoid is interpreted as the antorbital. The fifth infraorbital is a large plate, with a tubular relief for the infraorbital sensory canal, located near the orbital border of the bone. Posteriorly, the bone has a deep notch. The infraorbital canal has a straight tubule in right angle, extending posteriorly to the opercular series, as observed in *Apateodus striatus* (Newbrey and Konishi[25]: Fig. 3).

The upper jaw is composed by long and low premaxilla and maxilla. Both are poorly preserved and seem to be edentulous.

From the lower jaw, an elongate and triangular dentary is preserved. As the upper jaw bones, it is edentulous. The mandibular sensory canal is bone enclosed and runs along the dentary, close to its ventral border. The anguloarticular is a small bone with a partially preserved coronoid process, and a reduced postarticular process. The bone has a short anterior process to fit between the two branches of the dentary. Its posterior portion ends in a straight border. The mandibular sensory canal is bone enclosed and has single ventral pore externally. The quadrate facet is slightly excavated. Near this facet, there is a vertical strut probably to attach the *ligamentum primordium*. The Meckelian fossa is short and low, and its ventral border is strengthened by a bony crest. The retroarticular bone is not preserved.

Only the right side of the hyopalatine series is preserved, being marked by a forwardly inclination. The hyomandibula is a squarish and stout bone, bearing two articular heads. The condylar opercular process is thick and rounded, positioned posterodorsally. The ventral process is very reduced. There is a deep posterior excavation on the lateral face of the bone to the insertion of the *levator arcus palatine* muscle. The quadrate, triangular in shape, has a well-developed articular condyle with prominent mesial and lateral portions. The posteroventral process of the quadrate is strengthened and short, not surpassing the upper limit of the symplectic notch. Dorsally, the quadrate has a straight suture for the metapterygoid. The main body of the quadrate has a shallow fossa for the *adductor mandible* muscle. The anteroventral border of the bone has an outgrowth to receive the posterodorsal arm of the ectopterygoid. The symplectic is a large triangular bone inserted in a shallow notch in the quadrate. The metapterygoid is roughly trapezoidal and broad, bearing medially a stout process for contact with the basipterygoid process. The ectopterygoid is partially preserved like a long stick crossing the orbit. The endopterygoid is an elongate and spatulate bone without teeth. The palatine is elongated and triangular in lateral view, with a low dorsal keel that ventrally ends in an outer flat platform. The bone has a prominent anterior process filled with cartilage in life. It is toothless.

An elongated and low bony fragment displaced from the usual anatomical position is interpreted as a branchiostegal ray.

The urohyal is a very elongate bone, with a capitate anterior edge and a low keel. Its ventral edge is strengthened and finishes in and dilated posterior tip.

The opercle is deeper than long, but not an elliptical bone, as usually seen in dercetids. It is similar to that of *Cyranichthys ornatissimus* (cf. Taverne[25], p. 110, Fig. 4). It has a strengthened and straight anterior crest and a convex posterior border. There is a deep notch for digitiform process of the subopercle. The facet for the hyomandibular is shallow.

The preopercle is a narrow and boomerang-shaped bone strengthened in the median portion by a prominent crest, which lodges the preopercular sensory canal. This canal does not give off subsidiary branches. As in dercetids, this bone lacks a recumbent ventral spine.

The interopercle and subopercle are not preserved.

Some isolated bones are recognized as elements of the branchial arches, including pharyngobranchial, epibranchial, ceratobranchial and hypobranchial bones. Toothplates seem to be absent. There are many stick-like bones in association to the branchial arches, which are interpreted as gill rakers, suggesting filter feeding habit for *Antarctichthys*.

The first and second pharyngobranchials are small nodular bones, with two anterior bulges and a flattened main body. The first pharyngobranchial has a shallow posterior articular facet to receive the first epibranchial. The second pharyngobranchial is spool-like and larger than the first one. It is reduced to the perichondral covering. Its anterior tip produces an outgrowth with a deep excavation, which might receive the uncinate process of the second epibranchial.

The first and second epibranchials are tubular and elongate. The former is small and well-ossified, whereas the latter is large and hollow, probably filled with cartilage in life. The second epibranchial bears a small protuberance, herein interpreted as the process uncinated, which is recognized as a synapomorphy of Aulopiformes (cf.[5]).

The first and second ceratobranchials are rod-like and curved, bearing a longitudinal groove along the bone.

The second hypobranchial is large, elongate and slightly arched. It has an enlarged and capitate anterior tip.

The pectoral girdle includes post-temporal, cleithrum, coracoid and scapula; supracleithrum, postcleithrum and mesocoracoid were not observed. The left post-temporal is represented only by its spatulate dorsal arm displaced from the anatomical position. The left cleithrum is best preserved, whereas only the first third of the right one remains. The bone is large and has a strengthened crest all along its anterolateral border. Both arms are almost equal in length. The dorsal arm produces a short laminate outgrowth backwards. Its acute uppermost portion is broken and preserved laterally. Its ventral arm is laterally expanded in a wing, which tapers forwards forming a sharp anteroventral process.

The coracoid is a very large subrectangular plate with a convex outer surface and a deeply concave inner surface. Its posterodorsal border is broad to meet the scapula, whereas its anterodorsal border is slightly curved to contact the cleithrum tightly, so that the pectoral fenestra is absent. Anterior to the convex portion of the bone, there is a flat surface finishing in a deep and stout anterior process. All this outer surface is filled by *abductor superficialis* muscle in life and its ventral border produces a continuous lateral crest. The inner surface is marked by a rectilinear crest to the insertion of the *adductor profundus* muscle and a flat surface lodges bundles of the *arrector dorsalis* muscle.

The scapula is roughly trapezoid and its prominent glenoid edge articulates with the uppermost pectoral fin-ray. The scapular foramen is placed in the junction of scapula and cleithrum.

Both pectoral fins consist of at least seven very elongate and stout rays. All rays bear long and sharp proximal and curved processes associated to *abductor* and *adductor* muscles of the pectoral girdle and fin.

Only the left pelvic bone is preserved. It is triangular, elongated and narrow, being three times longer than wide, and tapers to a point anteriorly. The pelvic bone has a thickened medial support, suggesting a tight association with its partner. It is expanded posteriorly to produce the well-developed articulatory region for the pelvic fin- rays, which seems to be preserved crushed in the pelvic bone.

The preserved portion of the vertebral column consists of at least 20 vertebrae. All of them are abdominal, indicating that the fish had an elongate body. The centra are spoon-like, longer than high, and show a very large notochordal foramen. The neural arches are large and deep as the centra. Except for the first centrum, whose neural arches are autogenous and finish in a well-developed and short spine, the remaining centra are fused with their respective neural arches bearing short, thin, and very inclined neural spine. The first and second centra bear a unique well-developed wing-like transverse process and an ovoid outline. From the third to the last preserved centra, the anterior transverse process is enlarged and sharp, while the posterior transverse process is atrophied. There is an oblique bone bridge between centra and anterior transverse process for lodging ventral branch of spinal ganglion. The anteriormost vertebrae bear separate neural spines (bifid condition), whereas in the posteriormost the spines are medianly fused. Prezygapophysis is expanded in a wing-like and incurved projection, whereas postzygapophysis is low and very reduced. The neural canal is enclosed in the thin wall of the neural arch and its diameter equals that of the centrum.

At least, there are seven short, curved and grooved ribs, which extend to the eighth centrum. Apparently, they are associated to the bone bridge of the anterior transverse process.

Epineurals, epipleurals and supraneurals are not preserved.

Phylogenetic analysis

The phylogenetic analysis was based on the data matrix originally proposed by Silva & Gallo[1] and later modified by Alvarado-Ortega & Díaz-Cruz[10]. We chose to restrict the analysis to Dercetidae, following the assumption, supported by several authors (e.g.,[1,10,26]), that they constitute a monophyletic group. This focused approach was adopted to enable a more precise assessment of the phylogenetic position of *Antarctichthys*. In doing so, we removed 23 uninformative characters at the Dercetidae level and proposed five new characters. The final data matrix comprises 69 unordered and unweighted characters.

The analysis generated 52 most parsimonious trees, for which the Majority-rule consensus was applied (Fig. 2a). Low support indices indicate insufficient data for certain taxa, as well as high level of homoplasy in the dataset. Almost all values of bootstrap are lower than 50% (not labelled in the tree), indicating that taxonomic relationships between dercetids remain unresolved or weakly supported (see also the stratigraphic congruence indices in Table 1). Despite these challenges, the analysis revealed that *Antarctichthys* is the sister-genus to the late-diverging clade *Rhynchodercetis* plus *Hastichthys*.

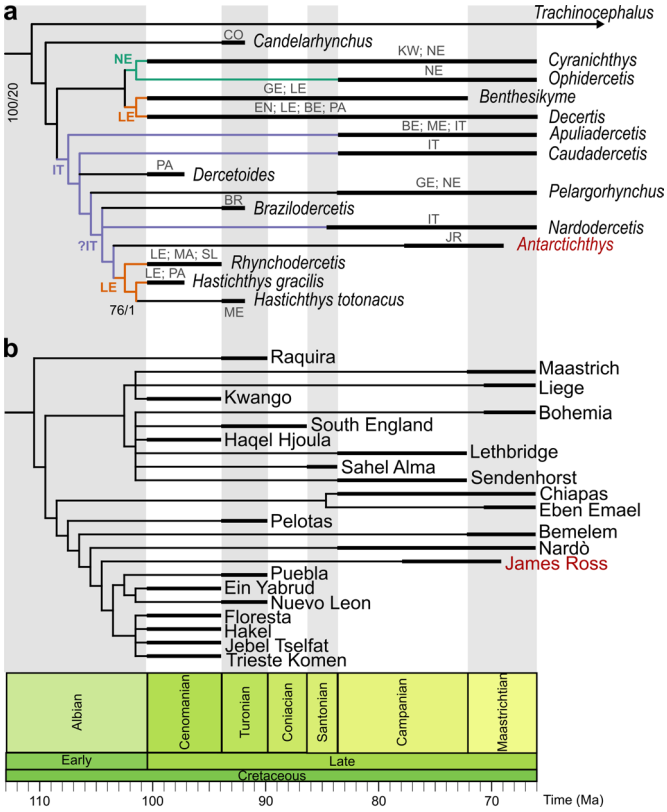

Fig. 2. Historical relationships of *Antarctichthys* among Dercetidae. (**a**) Majority-rule consensus of 52 most parsimonious trees with L = 166 steps, CI = 0.518 and RI = 0.490; (**b**) General area cladogram derived from BPA (Strict consensus of 6 most parsimonious trees with L = 32 steps, CI = 0.844 and RI = 0.940). Values at the nodes indicate Bootstrap/Bremer support (> 50%) where present. Colors indicate the inferred ancestral localities by congruence of taxa occurrences shown in (**a**). Each color is in accordance with the locality abbreviations. Abbreviations: BE, Belgium; BR, Brazil; CO, Colombia; EN, England; GE, Germany; IT¨, Italy; JR, James Ross (Antarctica); KW, Republic Democratic of the Congo; LE, Lebanon; MA, Morocco; ME, Mexico; NE, Netherlands; PA, Palestine; SL, Slovenia.

Tree sample	SRL	MIG	GMax	GMin	SCI	RCI	MSM*	GER	GER*	GERt	$p_{(SCI)}$	$p_{(RCI)}$	$p_{(GER)}$	$p_{(MSM)}$
IT	214.5	134.035	140.85	23.6	1	37.513	0.176	0.058	0.982	0.74	1.454×10^{-10}	0.009	0.972	0.351
RT	70.93	173.92	271.9	29.28	0.703	−144.628	0.167	0.162	–	–	–	–	–	–

Table 1. Obtained indexes of stratigraphic congruence analyses. GER, gap excess ratio; GER*, modification of GER considering the position of the input trees in the sample of randomly generated trees; GERt, modification of GER using the extreme values of MIGs from the random generated trees; GMax, the MIG of the worst fitted tree with the stratigraphy; GMin, the MIG of the tree with optimal fit to the stratigraphy; MIG, minimum implied gap; MSM, modified Manhattan stratigraphic measure; RCI, relative completeness index; SCI, stratigraphic consistency index; SRL, total simple range length. Abbreviations: IT, input tree; $p_{(GER)}$, estimated p-value for GER; $p_{(SCI)}$, estimated p-value for SCI; $p_{(MSM)}$, estimated p-value for MSM*; RT, median of the indexes obtained from random sampled trees.

Biogeographical analysis

We accomplished a Primary Brooks Parsimony Analysis (BPA[27]) to recover the distributional patterns of these fishes during the Late Cretaceous. Primary BPA is a valuable tool for identifying the most parsimonious general area cladogram based on a taxonomic cladogram and the geographic distributions of each terminal taxon. It also allows for testing whether vicariance alone can account for the observed biogeographic patterns[28]. The analysis yielded six most parsimonious trees, for which the strict consensus was applied, resulting in the general area cladogram (Fig. 2b). At the base of the cladogram, a primary cladogenetic event separates Ráquira (lower–middle Turonian, Colombia) from all other areas. Following this initial split, the remaining areas are organized into two distinct monophyletic groups. One of these groups forms a polytomy that includes Maastrich and Liège (both Maastrichtian, Belgium and Netherlands), along with Kwango (Cenomanian, Democratic

Republic of the Congo). The placement of Kwango within this clade may be influenced by sampling gap. The other polytomous group includes Sendenhorst (upper Cenomanian-Campanian, Germany, Czech Republic), Sahel Alma (upper Senonian, Lebanon), Lethbridge (upper Campanian, Canada), Haqel and Hjoula (upper Cenomanian, Lebanon), southeastern England (Senonian and Turonian), and Bohemia (Campanian, Czech Republic). Despite the temporal and geographic disparities among these areas, their clustering suggests possible historical biogeographical connections.

At the base of the second group lies a more resolved clade comprising Eben Emael (upper Maastrichtian, Belgium) and Chiapas (Campanian, Mexico), followed sequentially by Pelotas (lower Turonian, Brazil), Bemelen (Maastricthian, Netherlands), Nardò (Campanian–Maastrichtian, southern Italy) and James Ross Island (upper Campanian, Antarctica). There are two most apical clades. In one clade, Puebla (Turonian, Mexico) is the sister area to a grouping that includes Nuevo Leon (lower Turonian, Mexico) and Ein Yabrud (lower Cenomanian, Palestine); the other apical clade is a polytomy with Komen (lower Cenomanian, Slovenia), Jebel Tselfat (lower Cenomanian, Morocco), Haqel (upper Cenomanian, Lebanon) and Floresta (Cenomanian, Italy).

This hierarchical structure suggests complex biogeographical relationships among these areas, with varying degrees of divergence that likely reflect both temporal and spatial dynamics during the Late Cretaceous (Fig. 3).

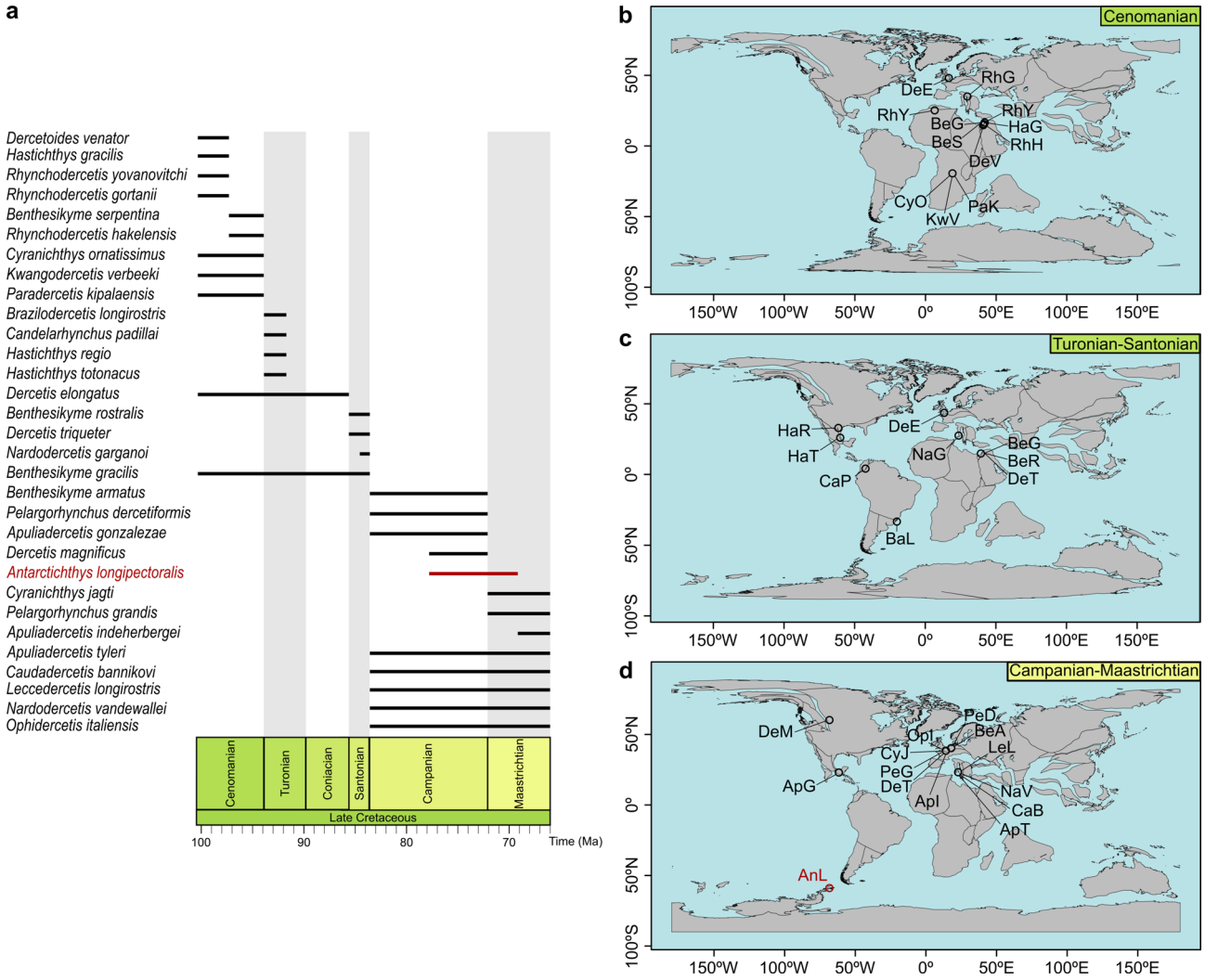

Fig. 3. Temporal range of dercetid species (**A**) and paleogeographical distribution in Cenomanian (**B**), Turonian–Santonian (**C**), Campanian–Maastrichtian intervals (**D**). Abbreviations: AnL, *Antarctichthys longipectoralis*; ApG, *Apuliadercetis gonzalezae*; ApI, *A. indeherbergei*; ApT, *A. tyleri*; BaL, *Brazilodercetis longirostris*; BeA, *Benthesikyme armatus*; BeG, *B. gracilis*; BeR, *B. rostralis*; BeS, *B. serpentina*; CaB, *Caudadercetis bannikovi*; CaP, *Candelarhynchus padillai*; CyJ, *Cyranichthys jagti*; CyO, *C. ornatissimus*; DeE, *Dercetis elongatus*; DeM, *D. magnificus*; DeT, *D. triqueter*; DeV, *Dercetoides venator*; HaG, *Hastichthys gracilis*; HaR, *H. regio*; HaT, *H. totonacus*; KwV, *Kwangodercetis verbeeki*; LeL, *Leccedercetis longirostris*; NaG, *Nardodercetis garganoi*; PaK, *Paradercetis kipalaensis*; NaV, *N. vandewallei*; OpI, *Ophidercetis italiensis*; PeD, *Pelargorhynchus dercetiformis*; PeG, *P. grandis*; RhG, *Rhynchodercetis gortanii*; RhH, *R. hakelensis*; RhY, *R. yovanovitchi*. Paleomaps obtained from the package *paleoMap*[52].

The basal placements and sequential arrangement within these clades provide insight into potential dispersal patterns and historical connections among these biogeographical zones.

Discussion

Antarctichthys longipectoralis is placed within Dercetidae due to the presence of their unequivocal synapomorphy: very reduced neural spines (their length equal or minus than half of the length of the vertebral centrum). Additionally, *Antarctichthys* bears features of the clade, including longirostrine head, very long and slender body, and large and deep neural arches on abdominal centra. Although the absence of a swimbladder was proposed as a synapomorphy of Aulopiformes[29], Baldwin & Johnson[5] did not recognized it as a derived feature of the clade. Given that ctenosquamates primitively have a swimbladder[5], it is possible that *Antarctichthys* had one, likely due to the presence of an otophysic connection.

Antarctichthys differs from all known dercetids by the absence of teeth, parietal ornamented with straight and parallel striae, presence of otophysic connection through exoccipital foramen, foramen for the glossopharyngeal nerve located near the contact zone between exoccipital and prootic, basioccipital with a long notochordal canal extending forward, and presence of very elongated and stout pectoral fin-rays.

When compared *Antarctichthys* to the dercetid genera included in the same clade (i.e., *Brazilodercetis*, *Nardodercetis*, *Rhynchodercetis* and *Hastichthys*), morphological distinctions are evident. *Brazilodercetis* differs by its medioparietal skull roof, pipe-like preopercle, elliptical opercle with conspicuous calathiform articular process, two pairs of wing-like transverse processes on each abdominal vertebra and tripartite scutes along the flank. *Nardodercetis* is distinguished by its large size, pelvic fins larger than the pectoral fins, and a row of tripartite scutes along the flank. *Rhynchodercetis* differs from *Antarctichthys* by reduced pectoral fins, two pairs of transverse processes on each vertebral centra and scutes along the flank. *Hastichthys* is set apart by its shorter snout, with lower jaw extending to anterior tip of snout, presence of interopercle, two pairs of transverse processes on each vertebral centra and a row of tripartite scutes along the flank.

The discovery of *Antarctichthys longipectoralis* adds a new dimension to our understanding of dercetid anatomy and the evolution of Aulopiformes during the Late Cretaceous. The presence of a well-developed otophysic connection, edentulous jaws, and unusually elongated pectoral fin-rays represent a unique anatomical configuration among dercetids, expanding the known morphological disparity within the group. These features also provide new characters for phylogenetic reconstructions and offer potential insights into ecological adaptations, such as specialized feeding strategies possibly related to filter feeding (Fig. 4). Phylogenetically, *Antarctichthys* occupies a pivotal position as sister-genus to *Rhynchodercetis* and *Hastichthys*, contributing to the resolution of relationships within the late-diverging clade of Dercetidae.

From a biogeographic standpoint, *Antarctichthys* represents the southernmost record of Dercetidae, highlighting a significant extension of their distribution into high-latitude marine ecosystems. Its occurrence in the Snow Hill Island Formation provides a rare glimpse into the fish fauna of the Antarctic during the Campanian and enables a qualitative comparison with contemporaneous fish faunas from lower latitudes. The assemblage from Antarctica, though still poorly known, shares affinities with Campanian–Maastrichtian faunas from South America and the Northern Hemisphere, suggesting complex distributional pattern and faunal exchanges across Tethyan and South Atlantic oceans. The Antarctic dercetid thus serves as a key taxon for future studies on Late Cretaceous marine biogeography and the evolutionary dynamics of teleost fishes during a time of significant global change.

Methods

Specimen

The material was collected by a team of researchers from the Museu Nacional (PALEOANTAR Project), on January 4 2019, encompassing an articulated aulopiform fish (field number: AF3P7BMN#38). This fish is preserved in a carbonate concretion and exhibit a well-preserved skull and an incomplete vertebral column. The holotype MN 7838-V is housed in the Paleovertebrate Collection, Departamento de Geologia e Paleontologia, Museu Nacional, Universidade Federal do Rio de Janeiro, Rio de Janeiro, RJ, Brazil.

Anatomical terms, counts and measurements follow Baldwin & Johnson[5], Beckett et al.[30] Figueiredo & Gallo[31], and Taverne[25].

Micro-computed tomographic-scan

The microCT was performed by a V|tome|x M with an X-ray microfocus computed tomography system (Baker and Huges GE) in the Instituto Alberto Luiz Coimbra de Pós-Graduação e Pesquisa de Engenharia (COPPE). Scan parameters were set at 180 kV voltage, 200 µA current, 500 ms exposure, 1 mm thick Al filter, 100 µm voxel size resolution, and a total of 1,500 projections in a 360° rotation. Phoenix Data X Reconstruction v. 2.2 (GE) was used for the 3D reconstructions, employing slice alignment, beam hardening correction, and ring artifact reduction. A mathematical edge enhancement filter was applied to obtain greater contrast of the structures. The images were treated in ImageJ 1.53t[32], resulting in 1,625 slices. We segmented the resulted images in 3DSlicer v.2.7.8[33].

Phylogenetic analysis

The systematic assignment of *Antarctichthys* within the monophyletic Dercetidae (sensu Alvarado-Ortega & Díaz-Cruz[10]) was performed with a phylogenetic analysis in TNT 1.6[34]. We have used the data set restricted to Dercetidae[10,26] (Additional information). The terminal taxa for the ingroup were *Antarctichthys*, *Apuliadercetis, Bentheskyme, Brazilodercetis, Candelarhynchus*, *Caudadercetis, Cyranichthys, Dercetis, Dercetoides, Hastichthys,*

Fig. 4. Life reconstruction of *Antarctichthys longipectoralis* gen. et sp. nov. and of the biota of Snow Hill Island Formation. Artwork of Maurilio Oliveira (2024).

Nardodercetis, Ophidercetis, Pelargorhynchus and *Rhynchodercetis*. Outgroup is based on the living Aulopiformes *Trachinocephalus*.

Regarding the small taxa data matrix (Additional information), we were able to apply an exhaustive search, using the implicit enumeration algorithm from TNT version 1.6. The memory available (General RAM) for the analysis was 500 MB, which enabled the program to hold 2,495,000 trees. The script 'STATS.-RUN' was used to retrieve consistency and retention indexes (CI and RI, respectively). We conducted Bootstrap resampling and Bremer support analyses to assess clade support.

As this is a genus-level phylogeny, the species chosen for the analysis were those whose data were obtained directly of the examined material deposited in selected paleontological collections (see Silva & Gallo[1], for a list of the analyzed material). Data concerning non-examined material (e.g., *Dercetoides* and *Hastichthys*) were obtained from original literature (e.g.,[35,36]).

Time-scaled phylogeny and stratigraphic congruence analyses

The obtained phylogenetic tree was time-calibrated in R v4.3.3[37]. We employed the packages *ape*[38] and *geiger*[39] to open and treat the parenthetical tree data. The calibration was performed by the *paleotree* package[40], by using the minimum branch length (mbl) method (the scripts are in Additional information). The resulted calibrated tree was plotted in the International Chronostratigraphic Chart (2013)[42], by *strap* package[42]. We performed the stratigraphic congruence analyses to evaluate its ghost lineages, available in *strap*. We excluded the living *Trachinocephalus* from these analyses due to be the unique extant lineage in the phylogeny, which strongly influences the ghost lineage evaluation indexes, and by our main goal being the evaluation of Dercetidae. Therefore, we considered *Candelarhynchus* as an outgroup in stratigraphic congruence analyses, due to its stable position as an early-diverging dercetid lineage. The number of sampled trees to be produced by resolving polytomies, as well as the number of random trees to be produced in calculating probabilities for the input trees were 50,000, as the recommended[43]. We employed the following indexes in our analyses: stratigraphy consistency index (SCI[44]); relative completeness index (RCI[45]); Manhattan stratigraphic measure (MSM[46], and its modification[47,48]); and Gap Excess Ratio (GER[49], and its modifications[43]). For randomization tests, we consider $\alpha = 0.05$.

Biogeographical analysis

BPA was performed based on the cladogram (Fig. 2), which was used to produce the taxon-area association. To generate an area cladogram, taxa were replaced by their corresponding areas. From this, an area matrix was constructed, in which each node represents a component, with the presence of an area coded as "1" and its absence as "0". A hypothetical area coded "0" was included to root the cladogram(s). The data matrix was analyzed using the implicit enumeration algorithm from TNT version 1.6.

Paleogeographic methods

The occurrences at species level were calibrated in deep time by the package *palaeoverse*[50]. The paleocoordinates were obtained by their stratigraphic horizons and its conversions in the Paleobiology Database[51]. The paleocoordinates were plotted in paleomaps—obtained from *paleomap*[52]—by the packages *broom*, *mapproj*, *ggthemes*, *sf*, and *tidyverse*.

Data availability

All data generated or analysed during this study are included in the following Supplementary material files: BPADercetidae, Matrix-dercetidae, CódigosFinal.zip. The data are also available in the Section "Supplementary information" at the end of this manuscript.

Received: 19 December 2024; Accepted: 21 May 2025
Published online: 11 August 2025

References

1. Silva, H. M. A. & Gallo, V. Taxonomic review and phylogenetic analysis of Enchodontoidei (Teleostei: Aulopiformes). *An. Acad. Bras. Ciênc.* **83**, 483–511 (2011).
2. Kriwet, J., Lirio, J. M., Nuñez, H. J., Puceat, E. & Lécuyer, C. Late Cretaceous Antarctic fish diversity. *Geol. Soc. Lond. Spec. Publ.* **258**, 83–100 (2006).
3. Goody, P. C. The relationships of certain Upper Cretaceous teleosts with special reference to the myctophoids. *Bull. Br. Mus. Nat. Hist. Geol.* **7**, 1–255 (1969).
4. Rosen, D. E. Interrelationships of higher euteleostean fishes. in *Interrelationships of fishes* 397–513 (Zoological Journal of the Linnean Society, London, 1973).
5. Baldwin, C. & Johnson, G. D. Interrelationships of Aulopiformes. in *Interrelationships of Fishes* 355–404 (Academic Press, San Diego, 1996).
6. Sato, T. & Nakabo, T. Paraulopidae and *Paraulopus*, a new family and genus of aulopiform fishes with revised relationships within the order. *Ichthyol. Res.* **49**, 25–46 (2002).
7. Nelson, J. S., Grande, T. C. & Wilson, M. V. H. *Fishes of the World*. (Wiley, 2016). https://doi.org/10.1002/9781119174844.
8. Chida, M., Brinkman, D. B. & Murray, A. M. A large, new dercetid fish (Teleostei: Aulopiformes) from the Campanian Bearpaw Formation of Alberta, Candada. *Cretac. Res.* **150**, 105579 (2023).
9. Taverne, L. & Goolaerts, S. The dercetid fishes (Teleostei, Aulopiformes) from the Maastrichtian (Late Cretaceous) of Belgium and The Netherlands. *Geol. Belg.* **18**, 21–30 (2015).
10. Alvarado-Ortega, J. & Díaz-Cruz, J. A. *Hastichthys totonacus* sp. nov., a North American Turonian dercetid fish (Teleostei, Aulopiformes) from the Huehuetla quarry, Puebla, Mexico. *J. S. Am. Earth Sci.* **105**, 102900 (2021).
11. Woodward, A. S. On fossil fish-remains from Snow Hill and Seymour Islands. *Lithogr. Inst. Gen.* **3**, 1–6 (1908).
12. Cione, A. L. & Medina, F. A. A record of *Notidanodon pectinatus* (Chondrichthyes, Hexanchiformes) in the Upper Cretaceous of the Antarctic Peninsula. *Mesoz. Res.* **1**, 79–88 (1987).
13. Grande, L. & Chatterjee, S. New Cretaceous fish fossils from Seymour Island, Antarctic Peninsula. *Palaeontology* **30**, 829–837 (1987).
14. Grande, L. & Eastman, J. T. A review of Antarctic ichthyofaunas in the light of new fossil discoveries. *Palaeontology* **29**, 113–137 (1986).
15. Martin, J. E. & Crame, J. A. Palaeobiological significance of high-latitude Late Cretaceous vertebrate fossils from the James Ross Basin. *Antarctica. Geol. Soc. Lond. Spec. Publ.* **258**, 109–124 (2006).
16. Otero, R. A. et al. A new species of chimaeriform (Chondrichthyes, Holocephali) from the uppermost Cretaceous of the López de Bertodano Formation, Isla Marambio (Seymour Island). *Antarctica. Antarct. Sci.* **25**, 99–106 (2013).
17. Otero, R. A. et al. New chondrichthyans from the Upper Cretaceous (Campanian–Maastrichtian) of Seymour and James Ross Islands, Antarctica. *J. Paleontol.* **88**, 411–420 (2014).
18. Reguero, M. A. et al. Late Campanian-Early Maastrichtian vertebrates from the James Ross Basin, West Antarctica: Updated synthesis, biostratigraphy, and paleobiogeography. *An. Acad. Bras. Ciênc.* **94**, e20211142 (2022).
19. Richter, M. & Thomson, M. R. A. First Aspidorhynchidae (Pisces: Teleostei) from Antarctica. *Antarct. Sci.* **1**, 57–64 (1989).
20. Richter, M. & Ward, D. J. Fish remains from the Santa Marta Formation (Late Cretaceous) of James Ross Island, Antarctica. *Antarct. Sci.* **2**, 67–76 (1990).
21. Stahl, B. J. & Chatterjee, S. A late cretaceous chimaerid (Chondrichthyes, Holocephali) from Seymour Island, Antarctica. *Palaeontology* **42**, 979–989 (1999).
22. Stahl, B. J. & Chatterjee, S. A Late Cretaceous callorhynchid (Chondrichthyes, Holocephali) from Seymour Island, Antarctica. *J. Vertebr. Paleontol.* **22**, 848–850 (2003).
23. Cione, A. L. et al. Before and after the K/Pg extinction in West Antarctica: New marine fish records from Marambio (Seymour) Island. *Cretac. Res.* **85**, 250–265 (2018).
24. Milanese, F. N. et al. Coniacian-Campanian magnetostratigraphy of the Marambio Group: The Santonian-Campanian boundary in the Antarctic Peninsula and the complete Upper Cretaceous—Lowermost Paleogene chronostratigraphical framework for the James Ross Basin. *Palaeogeogr. Palaeoclimatol. Palaeoecol.* **555**, 109871 (2020).
25. Taverne, L. Ostéologie de *Cyranichthys ornatissimus* nov. gen. du Cénomanien du Zaïre et de *Rhynchodercetis yovanovitchi* du Cénomanien de l'Afrique du Nord. Les relations intergénériques et la position systématique de la famille néocrétacique marine des Dercetidae (Pisces, Teleostei). *Ann. Mus. R. Afr. Cent. Rapp. Annu.* **1985–86**, 93–112 (1987).
26. Gallo, V., Figueiredo, F. J. & Silva, H. M. A. Análise filogenética dos Dercetidae (Teleostei, Aulopiformes). *Arq. Mus. Nac.* **63**, 329–352 (2005).
27. Brooks, D. R., Van Veller, M. G. P. & McLennan, D. A. How to do BPA, really. *J. Biogeogr.* **28**, 345–358 (2001).
28. Santos, C. M. D., Santos, D., Gois, J. P. & Hammoud, M. BuM 2.0: Software for online generation of matrices for Brooks Parsimony Analysis. *Zootaxa* **5005**, 241–245 (2021).
29. Johnson, G. D. Monophyly of the euteleostean clades: Neoteleostei, Eurypterygii, and Ctenosquamata. *Copeia* **1992**, 8 (1992).

30. Beckett, H., Giles, S. & Friedman, M. Comparative anatomy of the gill skeleton of fossil Aulopiformes (Teleostei: Eurypterygii). *J. Syst. Palaeontol.* **16**, 1221–1245 (2018).
31. Figueiredo, F. J. & Gallo, V. New dercetid fish (Neoteleostei: Aulopiformes) from the Turonian of the Pelotas Basin, Southern Brazil. *Palaeontology* **49**, 445–456 (2006).
32. Schneider, C. A., Rasband, W. S. & Eliceiri, K. W. NIH Image to ImageJ: 25 years of image analysis. *Nat. Methods* **9**, 671–675 (2012).
33. Kikinis, R., Pieper, S. D. & Vosburgh, K. G. 3D Slicer: A Platform for Subject-Specific Image Analysis, Visualization, and Clinical Support. in *Intraoperative Imaging and Image-Guided Therapy* (ed. Jolesz, F. A.) 277–289 (Springer New York, New York, NY, 2014). https://doi.org/10.1007/978-1-4614-7657-3_19.
34. Goloboff, P. A. & Morales, M. E. TNT version 1.6, with a graphical interface for MacOS and Linux, including new routines in parallel. *Cladistics* **39**, 144–153 (2023).
35. Chalifa, Y. Two new species of longirostrine fishes from the Early Cenomanian (Late Cretaceous) of Ein-Yabrud, Israel, with comments on the phylogeny of the Dercetidae. *J. Vertebr. Paleontol.* **9**, 314–328 (1989).
36. Taverne, L. New considerations on the osteology and phylogeny of the Cretaceous marine teleost family Dercetidae. *Biol. Jaarb. Dodonaea* **58**, 94–112 (1991).
37. R Core Team. R: A language and environment for statistical computing. R Foundation for Statistical Computing (2025).
38. Paradis, E. & Schliep, K. ape 5.0: an environment for modern phylogenetics and evolutionary analyses in R. *Bioinformatics* **35**, 526–528 (2019).
39. Pennell, M. W. *et al.* geiger v2.0: an expanded suite of methods for fitting macroevolutionary models to phylogenetic trees. *Bioinformatics* **30**, 2216–2218 (2014).
40. Bapst, D. W. paleotree: an R package for paleontological and phylogenetic analyses of evolution. *Methods Ecol. Evol.* **3**, 803–807 (2012).
41. Cohen, K. M., Finney, S. C., Gibbard, P. L. & Fan, J.-X. The ICS international chronostratigraphic chart. *Episodes* **36**, 199–204 (2013).
42. Bell, M. A. & Lloyd, G. T. strap: An R package for plotting phylogenies against stratigraphy and assessing their stratigraphic congruence. *Palaeontology* **58**, 379–389 (2015).
43. Wills, M. A., Barrett, P. M. & Heathcote, J. F. The modified gap excess ratio (GER*) and the Stratigraphic congruence of dinosaur phylogenies. *Syst. Biol.* **57**, 891–904 (2008).
44. Huelsenbeck, J. P. Comparing the stratigraphic record to estimates of phylogeny. *Paleobiology* **20**, 470–483 (1994).
45. Benton, M. J. & Storrs, G. Wm. Testing the quality of the fossil record: Paleontological knowledge is improving. *Geology* **22**, 111 (1994).
46. Siddall, M. E. Stratigraphic fit to phylogenies: A proposed solution. *Cladistics* **14**, 201–208 (1998).
47. Pol, D. Comments on the Manhattan stratigraphic measure. *Cladistics* **17**, 285–289 (2001).
48. Pol, D. & Norell, M. A. Uncertainty in the age of fossils and the stratigraphic fit to phylogenies. *Syst. Biol.* **55**, 512–521 (2006).
49. Boyd, C. A., Cleland, T. P., Marrero, N. L. & Clarke, J. A. Exploring the effects of phylogenetic uncertainty and consensus trees on stratigraphic consistency scores: a new program and a standardized method. *Cladistics* **27**, 52–60 (2011).
50. Jones, L. A. et al. palaeoverse: A community-driven R package to support palaeobiological analysis. *Methods Ecol. Evol.* **14**, 2205–2215 (2023).
51. The Paleobiology Database. The Paleobiology Database. [object Object] https://doi.org/10.15468/ZZOYXI (2024).
52. Leo, S. & Varela, S. paleoMap: An R-package for getting and using paleontological maps. (2015).

Acknowledgements

We extend our sincere thanks to the Conselho Nacional de Desenvolvimento Científico e Tecnológico (CNPq) for their support through the research fellowship grants (#308071/2022-0 to VG; #308515/2023-4 to MBS; #308707/2023-0 to AWAK), the post-doctoral scholarship (168270/2023-4 to ASB), and the INCT PALEOVERT grant (#406902/2022). We also gratefully acknowledge the Coordenação de Aperfeiçoamento de Pessoal de Nível Superior (CAPES) for the PROANTAR fellowship (# 88887.336584/2019-00 to ASB, 2019-2023) and the CNPq funding for the PALEOANTAR Project (#442677/2018-9 to AWAK). VG thanks FAPERJ (E-26/204.026/2024 to VG; E-26/201.095/2022 to AWAK)for the Scientist of Our State (CNE) fellowship. Special thanks to the Willi Henning Society for providing free access to the TNT software. The PALEOANTAR Project team expresses deep gratitude to the entire NApOc Ary Rongel military crew and the HU-1 helicopter squadron pilots for their invaluable logistical support during fieldwork on the Antarctic Peninsula. We also wish to thank alpinist Denni Morais for his assistance withcamping logistics and his support in fieldwork and fossil collection, as well as Gabriel Wailante and Fábio Loreto for their help with fieldwork and fossil collection during camping activities.

Author contributions

VG conducted anatomical descriptions and comparisons; designed and interpreted all the manuscript analyses; and led the manuscript writing. FJF conducted anatomical descriptions and comparisons; designed and interpreted the phylogenetic and biogeographical analyses; and contributed substantially to the manuscript writing. ASB collected the specimen; contributed to anatomical descriptions and comparisons; conducted segmentation of µCT-scan data; designed and interpreted stratigraphic congruence analyses; interpreted and contributed to the phylogenetic and biogeographical analyses; participated in manuscript writing. MBS assisted with µCT-scan and segmentation; authored the geological section; provided a substantive review of the manuscript. JMS coordinated the fieldwork and project oversight; authored the geological section; provided substantive manuscript review. AEPP collected the specimen; contributed to geological discussions; provided substantive manuscript review. RGF collected the specimen; coordinated the fieldwork; contributed to geological discussions; took a lead role in manuscript writing and review. RTL supported µCT-scan data acquisition; authored the µCT-scan protocols section; substantively reviewed the manuscript. OMOA performed the µCT-scan and contributed to data acquisition; authored the µCT-scan protocols section; provided a substantive manuscript review. AWAK managed project administration and coordination and provided a comprehensive manuscript review. All authors reviewed and approved the submitted version of the manuscript.

Competing interests

The authors declare no competing interests.

Additional information

Supplementary Information The online version contains supplementary material available at https://doi.org/10.1038/s41598-025-03570-y.

Correspondence and requests for materials should be addressed to V.G. or A.S.B.

Reprints and permissions information is available at www.nature.com/reprints.

Publisher's note Springer Nature remains neutral with regard to jurisdictional claims in published maps and institutional affiliations.